Applied Mathematics and Computation 411 (2021) 126502

Contents lists available at ScienceDirect

Applied Mathematics and Computation

journal homepage: www.elsevier.com/locate/amc

Bidirectional non-linear stretched flow of Williamson nanofluid with swimming of motile gyrotactic microorganisms

Ying-Qing Song[a], Sami Ullah Khan[b], M Ijaz Khan[c,d], Muhammad Awais[e], Aamar Abbasi[f], Qiu-Hong Shi[g,*]

[a] College of Science, Hunan City University, Yiyang 413000, P R China
[b] Department of Mathematics, COMSATS University Islamabad, Sahiwal 57000, Pakistan
[c] Department of Mathematics, Riphah International University, I-14, Islamabad 44000, Pakistan
[d] Nonlinear Analysis and Applied Mathematics (NAAM) Research Group, Department of Mathematics, Faculty of Science, King Abdulaziz University, P.O. Box 80257, Jeddah 21589, Saudi Arabia
[e] University institute of Biochemistry and Biotechnology, PMAS-Arid Agriculture University, Rawalpindi, Pakistan
[f] Department of Mathematics, University of Azad Jammu & Kashmir, Muzaffarabad 13100, Pakistan
[g] Department of Mathematics, Huzhou University, Huzhou 313000, P R China

ARTICLE INFO

Article history:
Received 6 May 2021
Revised 1 June 2021
Accepted 2 July 2021

Keywords:
Three-dimensional flow
Williamson nanofluid
Motile microorganisms
Numerical technique

ABSTRACT

The fields of material manufacture, graphic designing, information science, aerodynamics, plastic industry and biotechnology have been found to have a greater reliance on the phenomenon of fluid flow over three-dimensional realms. Consequently, this article has been focused to the study of Williamson nanofluid containing microorganisms over three-dimensional surface under the influence of magnetic field through bidirectional non-linearly stretched surface. To transform the set of nonlinear partial differential equations into ordinary differentials equations by using appropriate similarity transformation. These obtained fundamental ordinary differential equations are solved numerically by exploiting bvp4c process built-in MATLAB mathematical software. The presentation of the results has been made in form of graphs and tables to warrant the comparison between different scenarios. More specifically the parameters like temperature profile, velocity profile, motility of organisms, concentration profiles, Peclet numbers, Lewis number, Williamson parameters, material parameter, Brownian motion parameters, Rayleigh numbers and Prandtl number were presented as the graphical outcomes. The numerical data suggested that greater values of Schmidt number, thermophoresis parameters and Brownian motion reduce the coefficient of wall heat transfer. The study has its applications in transportation hypothesis that is utilized in many automotive and industrial processes. The field of industrial manufacturing has also many applications that consider flow over a bidirectional stretched surface. The current approach explores the cumulative effect of different physical features on the flow of Williamson fluid, and there is no such effort in the reviewed studies.

* Corresponding author.
E-mail address: shiqiuhong@zjhu.edu.cn (Q.-H. Shi).

https://doi.org/10.1016/j.amc.2021.126502
0096-3003/

1. Introduction

The nanofluids have been found worthy during energy crises of the century in modern world as they possess ultra-high thermo-physical properties. These perilous and concurrent issues of energy crisis and energy conservation have been recently addressed by scientists of this era. The foremost idea of thermal efficacy improvement was put forward by Choi and Eastman [1] by adding nanomaterials to the subjected solution types. Many of the industrial processes involving heat transfer have been highly benefitted from Nanotechnology and the developments in the field of heat and mass transfer. More specifically, these fields include industrial biotechnology, drug development, nano-pharmaceutics, avionics, refrigeration and thermal control panels. Buongiorno [2] proposed the idea of using heterogeneous nanofluids to offer high throughput for convective processes involving heat transfer boundaries. Ramzan et al. [3] conducted a study to explore nanofluid flow over a curved surface with nonlinear thermal radiation involving autocatalytic chemical reaction and slip condition. The effects of radiative and peristaltic propulsion on heat transfer augmentation involving magnetic field were investigated by Katta and Jayavel [4]. Mustafa Turkyilmazoglu [5] explored the linear stability of single phase nanofluid and fluid spectacles. The Hafnium nanoparticles slip importance was investigated by Ellahi et al. [6]. Li et al. [7] examined the melting procedure to draw a numerical investigation of nanofluid influence involving this process. Qayyum et al. [8] examined the optimized entropy features in flow of Williamson nanofluid between rotating disks. Ibrahim [9] inspected the nanofluid analysis for tangent hyperbolic fluid subject to the slip mechanism. Ashraf et al. [10] discussed the peristaltic motion of blood based nanofluid containing the magnetite nanoparticles. Khan [11] analyzed the Darcy Forchheimer flow of hybrid nanofluid confined by rotating disk. The stability analysis in single phase nanofluid has been comprehensively discussed by Turkyilmazoglu [12]. Khan and Alzahrani [13] visulzied the nonlinear mixed convection flow of Carreau nanofluid with applications of activation energy. Ibrahim and Khan [14] examined the thermal aspects of SWCNT-Water and MWCNT-Water nanoparticles due to stretched surface.

Magnetohydrodynamic (MHD) flow research for nanofluids over three dimensional surfaces has been a key area of application and investigation for motivated scientists studying various industries and engineering fields involving material synthesis, condensation, polymer extrusion, paper manufacturing, polystyrene production, glass blowing and so on. Atif et al. [15] investigated heterogeneous bio-convective fluid crafted with gyrostatic microorganisms and nanoparticles. A similar study involving magnetohydrodynamic (MHD) flow with mixed microorganisms and nanoparticles fluid over stretching surface was studied by Hosseinzadeh et al. [16].

The bioconvection phenomena studies the random stratification governed upward flow of microorganisms in a solutions of variable density strata. This phenomena has been found to have its marvels in the fields of targeted drug delivery, biosensors, biotechnology, bio-fules, industrial manufacturing, avionics, material science and other engineering disciplines. Waqas et al. [17] explored the time dependent MHD flow of Williamson nanofluid for its heat and mass transfer involving motile microorganism. The Oldroyd-B nanofluid flow has been the point of discussion in the study conducted by Khan et al. [18] involving thermal radiation and motile. Alshomrani et al. [19] investigated a stretching cylinder shape dispensed in nanofluid under the influence of the ferromagnetic dipole. The further investigations of magnetized nanoparticle bioconvection were investigated by Alwatban et al. [20]. Tlili et al. [21] presented a study of Oldroyd-B fluid for its activation energy and second-order bioconvection slip. Waqas et al. [22] conducted the study that involved control the numerical mechanism of disk stretching relating electromagnetic nature of viscous nanofluid. Ramzan et al. [23] explored flow of nanofluid flow with Hall and Ion slip upshot combined with activation energy, gyrotactic microorganisms, and CattaneoChristov heat flux.

This contribution announces a new mathematical formulation for the flow of Williamson nanofluid flow through sheet with the impacts of magnetic field and motile microorganisms. The leading momentum, energy and concentration motile concentration equations are abridged into dimensionless forms as ordinary differential equations by implementing the similarity tactic. The numerical result of the problem is attained with the bvp4c algorithm in MATLAB mathematical software. The outcomes of numerous prominent foremost parameters are documented graphically and deliberated.

2. Mathematical model

A three-dimensional flow of Williamson nanofluid is examined in presence of gyrotactic microorganisms. For incompressible fluid flow, cartesian coordinate is followed to model the flow problem. Let u_1,u_2 and u_3 be velocity components along x_1,x_2 and x_3, respectively. The magnetic force impact is considered along x_3 direction foe the three-dimensional flow configuration. Let T be nanofluid temperature, C concentration and N motile density. The flow equations for current bio-convective flow problem are [8, 16]:

$$\frac{\partial u_1}{\partial x_1}+\frac{\partial u_2}{\partial x_2}+\frac{\partial u_3}{\partial x_3}=0, \tag{1}$$

$$u_1\frac{\partial u_1}{\partial x_1}+u_2\frac{\partial u_1}{\partial x_2}+u_3\frac{\partial u_1}{\partial x_3}=\nu\frac{\partial^2 u_1}{\partial x_3^2}+\sqrt{2\nu}\Gamma\frac{\partial u_1}{\partial x_3}\frac{\partial^2 u_1}{\partial x_3^2}-\frac{\sigma\beta_a^2}{\rho_f}u_1 + \frac{1}{\rho_f}\left[\begin{matrix}\left(1-C_f\right)\rho_f\beta^{**}g^*(T-T_\infty)-\left(\rho_p-\rho_f\right)g^*(C-C_\infty)\\ -(N-N_\infty)g^*\gamma\left(\rho_m-\rho_f\right)\end{matrix}\right], \tag{2}$$

$$u_1\frac{\partial u_2}{\partial x_1}+u_2\frac{\partial u_2}{\partial x_2}+u_3\frac{\partial u_2}{\partial x_3}=\nu\frac{\partial^2 u_2}{\partial x_3^2}+\sqrt{2\nu}\Gamma\frac{\partial u_2}{\partial x_3}\frac{\partial^2 u_2}{\partial x_3^2}-\frac{\sigma\beta_a^2}{\rho_f}u_2, \tag{3}$$

$$u_1\frac{\partial T}{\partial x_1}+u_2\frac{\partial T}{\partial x_2}+u_3\frac{\partial T}{\partial x_3}=a^*\frac{\partial^2 T}{\partial x_3^2}+\chi^*\left[D_B\frac{\partial C}{\partial x_3}\frac{\partial T}{\partial x_3}+\frac{D_T}{T_\infty}\left(\frac{\partial T}{\partial x_3}\right)^2\right], \tag{4}$$

$$u_1\frac{\partial C}{\partial x_1}+u_2\frac{\partial C}{\partial x_2}+u_3\frac{\partial C}{\partial x_3}=D_B\frac{\partial^2 C}{\partial x_3^2}+\frac{D_T}{T_\infty}\frac{\partial^2 T}{\partial x_3^2}, \tag{5}$$

$$u_1\frac{\partial N}{\partial x_1}+u_2\frac{\partial N}{\partial x_2}+u_3\frac{\partial N}{\partial x_3}+\frac{bW_c}{(C_w-C_\infty)}\left[\frac{\partial}{\partial x_3}\left(N\frac{\partial C}{\partial x_3}\right)\right]=D_m\left(\frac{\partial^2 N}{\partial x_3^2}\right) \tag{6}$$

with boundary conditions:

$$\begin{aligned}&u_1=a(x_1+x_2)^n, u_2=b(x_1+x_2)^n, u_3=0, -k\frac{\partial T}{\partial x_3}=h_f(T_w-T),\\ &D_B\frac{\partial C}{\partial x_3}+\frac{D_T}{T_\infty}\frac{\partial T}{\partial x_3}=0 \quad at \quad x_3=0,\\ &u_1\to 0, u_2\to 0, T\to T_\infty, C\to C_\infty, N\to N_\infty \ \ as \ \ x_3\to\infty,\end{aligned} \tag{7}$$

Let us assume prominent variables:

$$\begin{aligned}&u_1=\varepsilon af'(\zeta), u_2=\varepsilon bg'(\zeta), u_3=-\sqrt{a\nu}(x_1+x_2)^{\frac{n-1}{2}}\left(\frac{n+1}{2}(f+g)+\frac{n-1}{2}\zeta\left(f'+g'\right)\right),\\ &\theta(\zeta)=\frac{T-T_\infty}{T_w-T_\infty}, \phi(\zeta)=\frac{C-C_\infty}{C_\infty}, \chi(\zeta)=\frac{N-N_\infty}{N_\infty}\zeta=\sqrt{\frac{a}{\nu}}x_3(x_1+x_2)^{\frac{n-1}{2}}, \varepsilon=(x_1+x_2)^n.\end{aligned} \tag{8}$$

The governing equations in dimensionless form are:

$$f'''+\left(\frac{n+1}{2}\right)\left(f'+g'\right)f''-n\left(f'+g'\right)f'+Wef''f'''-Mf'+\lambda(\theta-Nr\phi-Nc\chi)=0 \tag{9}$$

$$g'''+\left(\frac{n+1}{2}\right)\left(f'+g'\right)g''-n\left(f'+g'\right)g'+Weg''g'''-Mg'=0 \tag{10}$$

$$\theta''+\left(\frac{n+1}{2}\right)(f+g)\theta'+Nb\theta'\phi'+Nt\left(\theta'\right)^2=0 \tag{11}$$

$$\phi''+\Pr Le\left(\frac{n+1}{2}\right)(f+g)\phi'+\frac{Nt}{Nb}\theta''=0, \tag{12}$$

$$\chi''+Lb\left(\frac{n+1}{2}\right)(f+g)\chi'-Pe\left(\phi''(\chi+\delta_1)+\chi'\phi'\right)=0. \tag{13}$$

$$\begin{aligned}&f(0)=0, f'(0)=1, g(0)=0, g'(0)=\alpha,\\ &Nb\phi'(0)+Nt\theta'(0)=0, \theta'(0)=-Bi\,(1-\theta(0))\\ &f'(\infty)\to\infty, g'(\infty)\to\infty, \theta(\infty)\to 0, \phi(\infty)\to 0, \chi(\infty)\to 0,\end{aligned} \tag{14}$$

with Brownian motion parameter $Nb=\frac{\chi^* D_B C_\infty}{\nu}$, thermophoresis parameter $Nt=\frac{\chi^* D_T(T_w-T_\infty)}{T_\infty\nu}$, stretching ratio parameter $\alpha=\frac{b}{a}$,the Prandtl number $\Pr=\frac{\nu}{a^*}$, The magnetic parameter $M=\frac{\sigma\beta_a^2}{\rho_f}a(x_1+x_2)^n$, $\lambda=\frac{\beta^{**}g^*(1-C_\infty)(T_f-T_\infty)}{aU_w}$ mixed convection parameter, $Nr=\frac{(\rho_p-\rho_f)(C_w-C_0)}{(1-C_\infty)(T_w-T_0)}$ buoyancy ratio parameter and bioconvection Rayleigh number $Nc=\frac{\gamma^*(\rho_m-\rho_f)(N_w-N_0)}{(1-C_\infty)(T_w-T_0)\beta^{**}}$. Biot number $Bi=\frac{h_f}{k}\sqrt{\frac{\nu}{a}}$, bioconvection Lewis number $Lb=\frac{\nu}{D_m}$,Peclet number $Pe=\frac{bW_c}{D_m}$and $Le=\frac{\alpha}{D_B}$ Lewis number respectively.

Demonstration of Skin friction coefficient and local Nusselt number are given as

$$\left.\begin{aligned}&Cfx_1=\frac{\tau_{x_3x_1}}{\rho_f u_w^2}, Cfx_2=\frac{\tau_{x_3x_2}}{\rho_f v_w^2} Nu_{x_1}=\frac{(x_1+x_2)q_w}{k(T_w-T_\infty)},\\ &\tau_{x_3x_1}=\frac{\partial u_1}{\partial x_3}+\frac{n\Gamma}{\sqrt{2}}\left(\frac{\partial u_1}{\partial x_3}\right)^2, \tau_{x_3x_1}=\frac{\partial u_2}{\partial x_3}+\frac{n\Gamma}{\sqrt{2}}\left(\frac{\partial u_2}{\partial x_3}\right)^2\end{aligned}\right\} \tag{15}$$

The skin friction coefficient and Nusselt number are arranged as

$$\begin{aligned}&C_f\mathrm{Re}_x^{-\frac{1}{2}}=f''(0)+We\left(f''\right)^2(0), C_g\mathrm{Re}_x^{\frac{1}{2}}=g''(0)+We\left(g''\right)^2(0)\\ &Nu_x\mathrm{Re}_x^{-\frac{1}{2}}=-\theta'(0).\end{aligned} \tag{16}$$

Here, $\mathrm{Re}_x=\frac{U_w(x_1+x_2)}{\nu}$ the local Reynolds numbers.

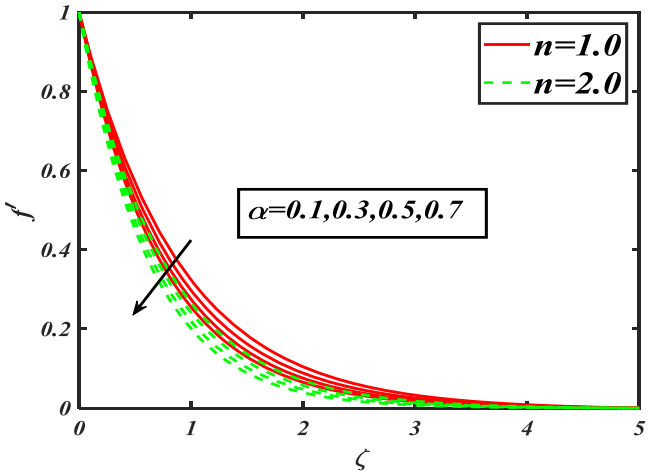

Fig. 1. fluctuation of velocity f' againstα.

3. Numerical scheme

The non-dimensional flow leading Eqs. (9-13) along with apposite boundary conditions (14) are elucidated numerically by exploiting bvp4c procedure.The higher order of derivative is abridged to a set of first order derivatives.

$$\left.\begin{array}{l} f = q_1,\ f' = q_2,\ f'' = q_3,\ f''' = q'_3,\ g = q_4,\ g' = q_5, \\ g'' = q_6,\ g''' = q'_6,\ \theta = q_7,\ \theta' = q_8,\ \theta'' = q'_8,\ \phi = q_9, \\ \phi' = q_{10},\ \phi'' = q'_{10},\ \chi = q_{11},\ \chi' = q_{12},\ \chi'' = q'_{12} \end{array}\right\} \tag{17}$$

$$q'_3 = \frac{n(q_2+q_5)q_2 - \left(\frac{n+1}{2}\right)(q_2+q_5)q_3 + Mq_2}{1+Weq_3} \tag{18}$$

$$q'_6 = \frac{n(q_2+q_5)q_5 - \left(\frac{n+1}{2}\right)(q_2+q_5)q_6 + Mq_5}{1+Weq_5} \tag{19}$$

$$q'_8 = -\Pr\left(\in q_8 + \left(\frac{n+1}{2}\right)(q_1+q_4)q_8 + Nbq_8q_{10} + Nt(q_8)^2\right), \tag{20}$$

$$q'_{10} = -\Pr Le\left(\frac{n+1}{2}\right)(q_1+q_4)q_{10} - \frac{Nt}{Nb}q'_8, \tag{21}$$

$$q'_{12} = -Lb\left(\frac{n+1}{2}\right)(q_1+q_4)q_{12} + Pe\left(q'_{10}(q_{11}+\delta_1) + q_{12}q_{10}\right) \tag{22}$$

$$\begin{array}{l} q_1(0) = 0, q_2(0) = 1, q_4(0) = 0, q_5(0) = \alpha, q_7(0) = 1, \\ Nbq_{10}(0) + Ntq_8(0) = 0, q_8(\zeta) = -Bi\,(1 - q_7(\zeta)) \\ q_2(\infty) \to \infty, q_5(\infty) \to \infty, q_7(\infty) \to 1, q_9(\infty) \to 0, q_{11}(\infty) \to 0, \end{array} \tag{23}$$

4. Results and discussion

In this section, Figs. 1-18 are outlined to discuss the impact of various flow parameters on the velocity, temperature, concentration and motile microorganisms. The plot in Fig. 1 explains the velocity fieldf' and stretching ratio parameter αrelationship that explain escalating values of α decreases the velocity of fluid $f'$for both cases of linear stretching and non-linear stretching surfaces. Fig. 2 presents magnetic parameter$M$and velocity profilef'relationships and it is perceived from the plots that velocity of nanofluid f' is reducing with increasing magnetic profile under both cases($n = 1\&2$). Fig. 3 is the representation of Rayleigh numberNc correlation with radial velocity f' involving linear and nonlinear stretched surfaces. The results clearly indicate that under both cases of linear and nonlinear stretching surfaces ($n = 1\&2$) high variation of bioconvection Raleigh number diminishes velocity concentration. The effect of mixed convection λon radial velocity field f' are studied and presented in Fig. 4. It is figured out from the results that for linear as well as nonlinear cases ($n = 1\&2$)

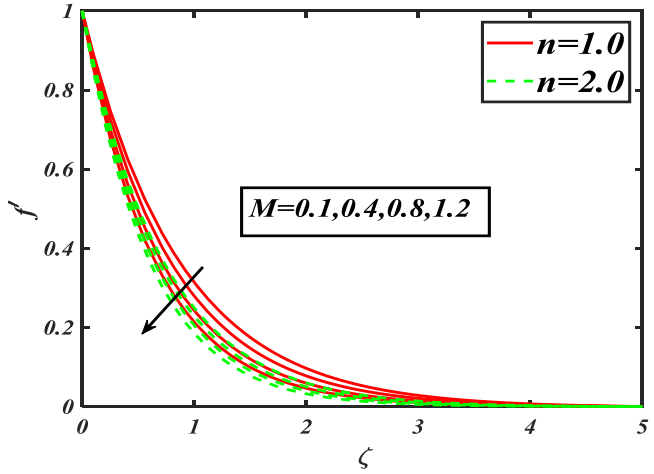

Fig. 2. fluctuation of f' against M.

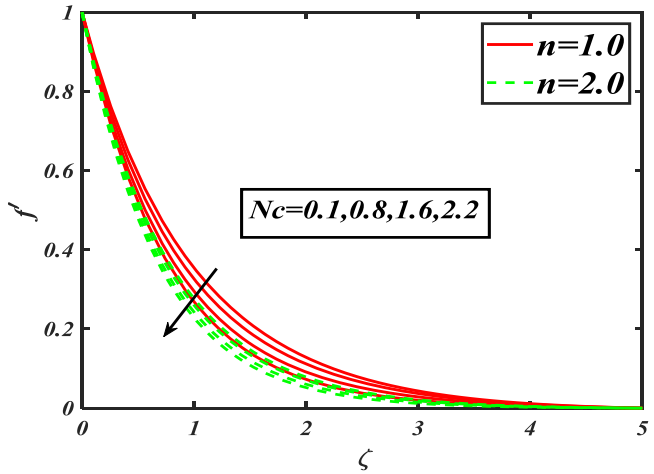

Fig. 3. fluctuation of velocity f' against Nc.

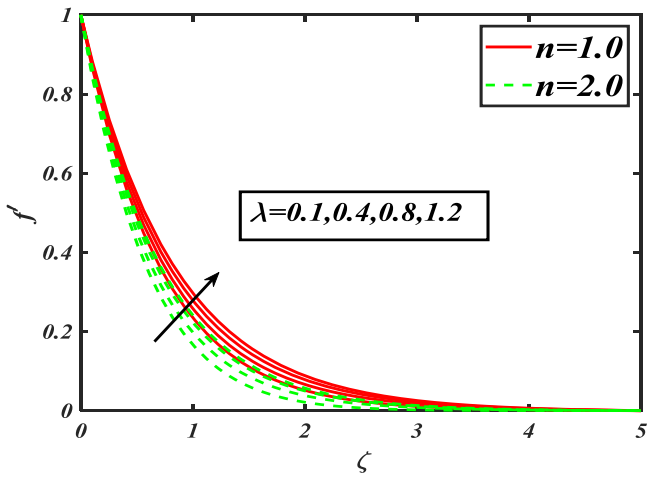

Fig. 4. fluctuation of velocity f' against λ.

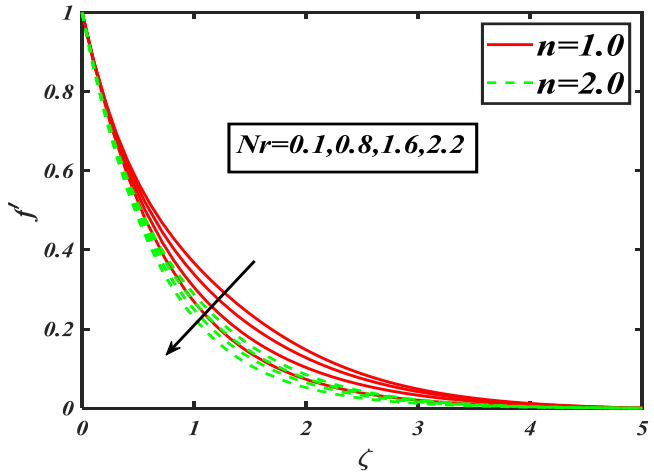

Fig. 5. fluctuation of velocity f against Nr.

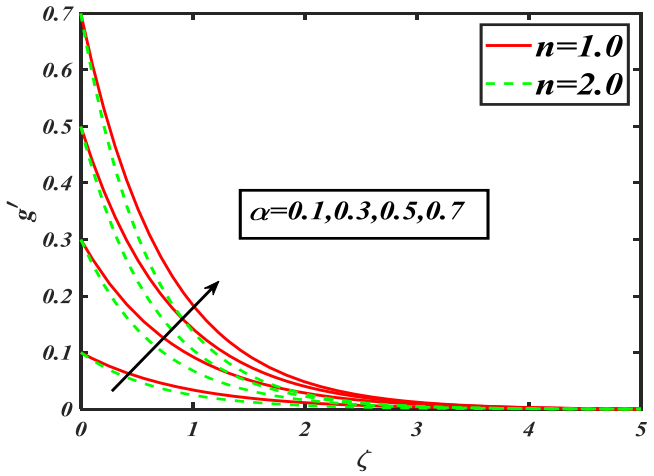

Fig. 6. fluctuation of velocity g'against α.

the radial velocity of fluid $f'$is intensified by the higher mixed convection values. Fig. 5 unveil the results of buoyancy ratio parameterNron velocity profile f' and a very clear observation is indicated in both linear and nonlinear cases $(n = 1\&2)$ that radial velocity of fluid f' is abridged by augmenting values of buoyancy ratio. Fig. 6 illustrates an association between stretching ratio parameter $\alpha$and velocity fieldf'. The results designate that escalating value of stretching parameter the azimuthal velocity of fluid $f'$is impeded in both cases$(n = 1\&2)$.

The Fig. 7 depicts magnetic parameter M association with azimuthal velocity concentration$g'$for both cases$(n = 1\&2)$. The curves indicate that azimuthal velocity f'sheds along with striking variation of magnetic parameter. The Biot number Biagainst temperature concentration θ are presented in Fig. 8 and it can be inferred that inflating Biot number values amended the temperature distribution for both scenarios$(n = 1\&2)$. Fig. 9 has been added to show the link of temperature profile θ for Prandtl numberPr in both cases$(n = 1\&2)$. It can be observed from the results that temperatureθ decays with rising variations of Prandtl numberPr. Fig. 10 is an explanation to the relationship of temperature field of nanoparticlesθ and stretching ratio parameterα. The results indicate diminishing of temperature field of nanoparticles by increasing stretching ratio for both cases linear stretching and nonlinear stretching. Fig. 11 attributes the Prandtl numberPr association with concentration field of nanoparticles$\varphi$for both cases linear stretching and nonlinear stretching. The hype in Prandtl number is found to be associated with a depletion of concentration fieldφ. The prominent bond between Brownian motion parameterNb and concentration field $\varphi$is presented in Fig. 12 that specifies a drop in concentration field φ advancement of Brownian motion parameter for both cases$(n = 1\&2)$. The volumetric concentration field$\varphi$and the nature of thermophoresis parameter Ntattachment is explained in Fig. 13. The findings indicate a surge in variation of thermophoresis parameter increment volumetric concentration of nanoparticlesφ. Fig. 14 elucidates the consequences associated with Lewis numberLe

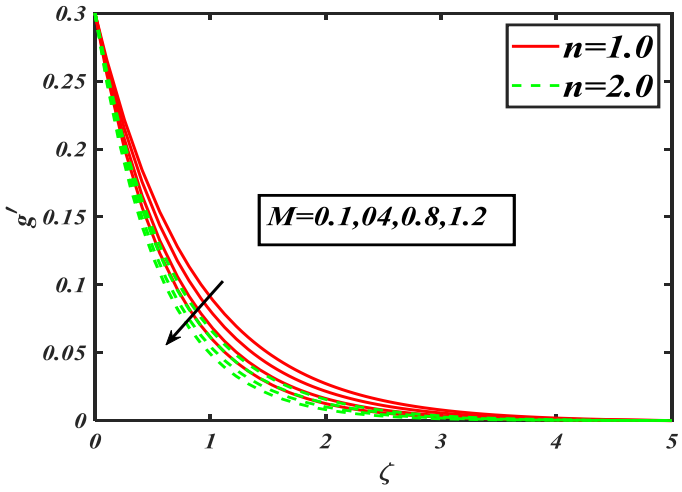

Fig. 7. fluctuation of velocity g'against M.

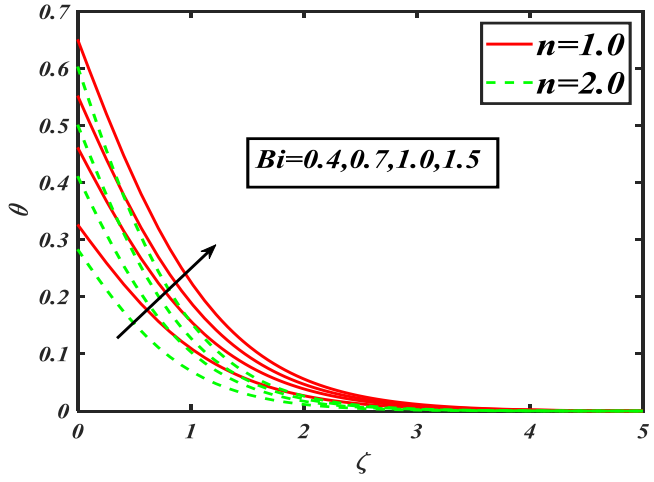

Fig. 8. fluctuation of velocity θagainst Bi.

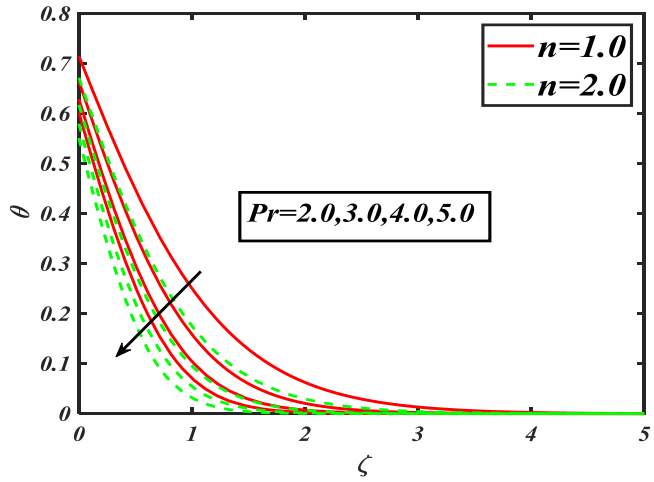

Fig. 9. fluctuation of velocity θagainst Pr.

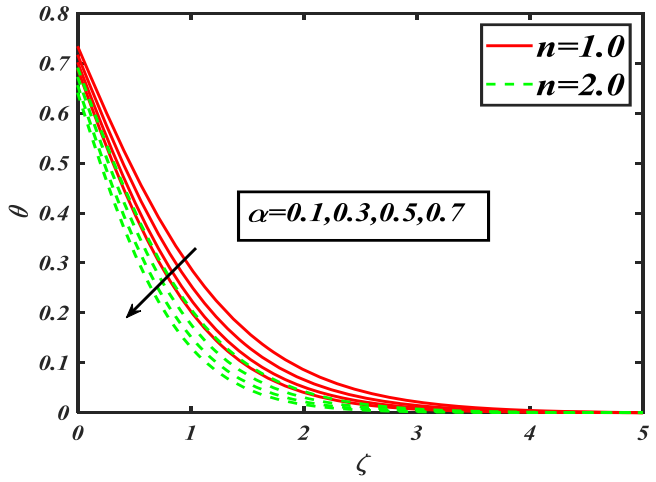

Fig. 10. fluctuation of velocity θagainst α.

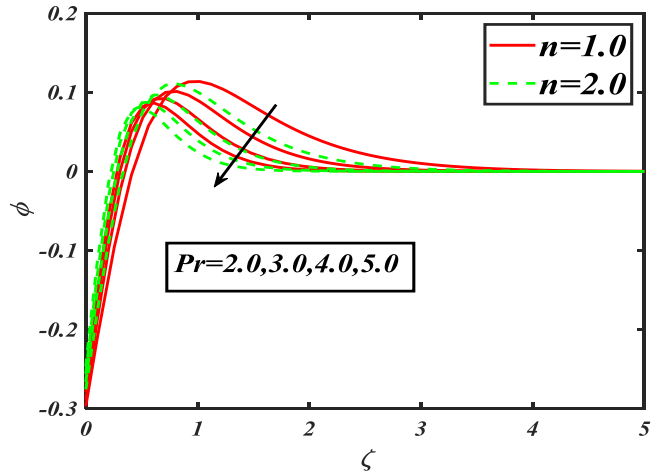

Fig. 11. fluctuation of velocity φagainst Pr.

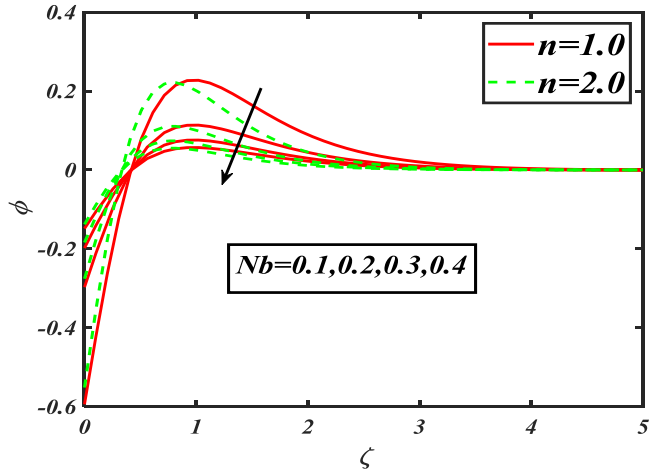

Fig. 12. fluctuation of velocity φagainst *Nb*.

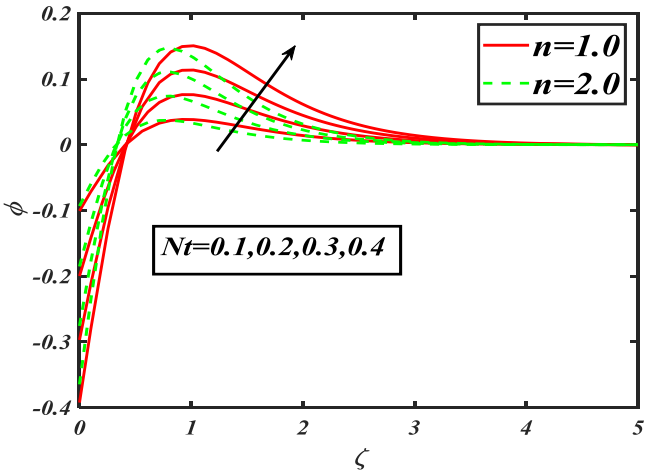

Fig. 13. fluctuation of velocity φagainst *Nt*.

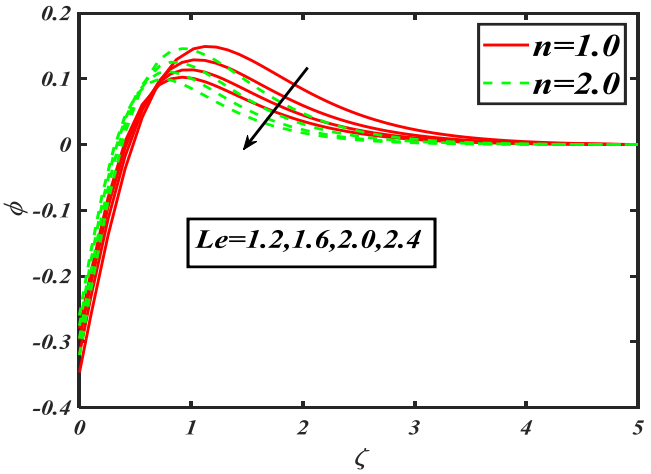

Fig. 14. fluctuation of velocity φagainst *Le*.

and concentration profile of nanoparticlesφ. The concentration field depletes with increasing variation of Lewis number*Le* for both values of$(n = 1\&2)$. Fig. 15 portraits the attachment of nature of stretching ratio parameterα and concentration field of nanoparticlesφ. The stretching ratio parameter enhancement in both linear and nonlinear cases$(n = 1\&2)$ is found to deplete the concentration field of nanoparticles. The findings of Peclet number *Pe* versus microorganism's concentration field$\chi$are presented in Fig. 16 that conclude the deterioration of microorganism's field χ augmenting Peclet number. Fig. 17 explains the link of bioconvection Lewis number *Lb*with the microorganism's concentration fieldχ. The findings specify that higher value of Lewis number are associated with decline in the microorganism's field χ for linear stretching and nonlinear stretching$(n = 1\&2)$. The Fig. 18 draft stretching ratio parameter α devotion with microorganism's concentration fieldχ for linear stretching and nonlinear stretching$(n = 1\&2)$. It is clearly observed that microorganism's field χ declines for progressive values of stretching ratio parameter.

Table 1 presents the outcomes associated with velocity parameter against the controlling parameters such as mixed convection, Prandtl number, and magnetic parameter. These results suggest that higher values of Raleigh number impede the variation of bioconvection. Table 2 explains the azimuthal velocity and the consequences of rolling prominent parameters. Table 3 describes temperature concentration in relationship with the characteristics of governing parameters. Table 4 reveals concentration profile parameter association with Raleigh number, magnetic parameter and mixed convection. Table 5 discloses the nature of motile microorganism's concentration for bioconvection Lewis number and Peclet number.

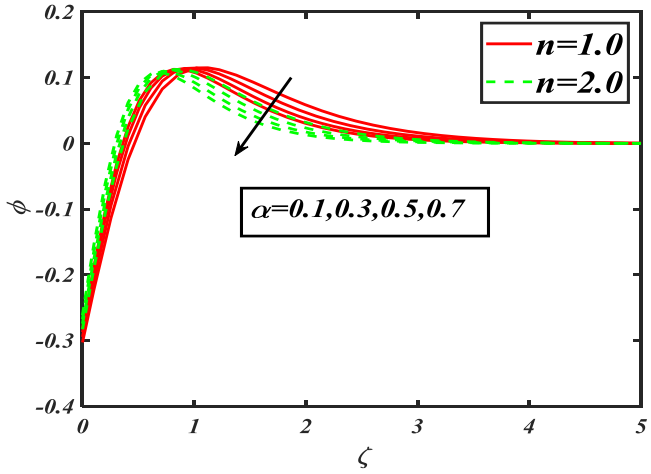

Fig. 15. fluctuation of velocity φagainst α.

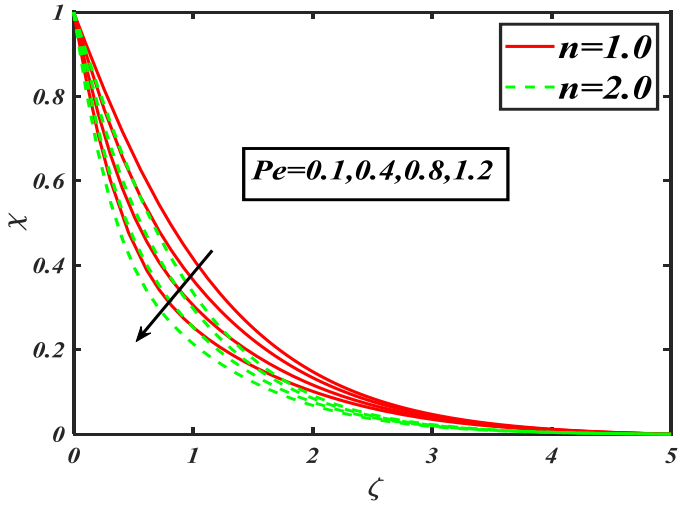

Fig. 16. fluctuation of velocity χagainst Pe.

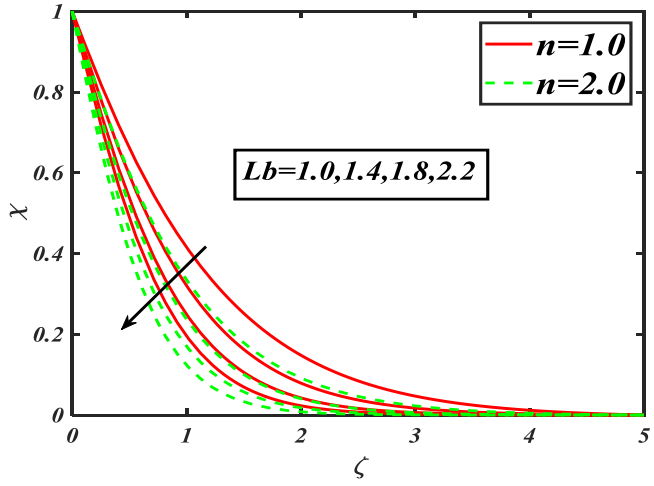

Fig. 17. fluctuation of velocity χagainst *Lb*.

Table 1
Outcomes $-f''(0)$ versus $M, \lambda, Nr, Nc, \Pr$ for both values of $n = 1$and $n = 2$..

Parameters						$-f''(0)$
M	λ	Nr	Nc	Pr	$n = 1$	$n = 2$
0.1	0.4	0.4	0.2	0.4	0.83741	1.17556
0.3					0.90768	1.22654
0.5					0.9996	1.35677
0.2	0.1	0.1			0.8538	0.97768
	0.3				0.8804	0.99786
	0.7				0.9442	1.04674
		0.3			0.9960	1.2547
		0.5			0.9358	1.0543
		0.9			0.8555	0.9545
			0.1		0.883928	0.99675
			0.5		0.85864	0.95764
			0.7		0.82736	0.90754
				0.3	0.95764	1.18756
				0.5	0.92957	0.99983
				0.9	0.91858	0.95276

Table 2
Outcomes of $-g''(0)$ versus $M, \lambda, Nr, Nc, \Pr$ for both cases linear and nonlinear stretching surface.

Parameters						$-g''(0)$
M	λ	Nr	Nc	Pr	$n = 1$	$n = 2$
0.2	0.3	0.3	0.3	0.5	0.45963	0.4276
0.4					0.480563	0.45675
0.8					0.51561	0.483675
0.3	0.2	0.1	0.1		0.52743	0.45566
	0.6				0.55653	0.47667
	0.8				0.58565	0.49997
0.2	0.3	0.2	0.1		0.504346	0.465768
		0.4			0.554355	0.49876
		0.6			0.656546	0.50675
0.2	0.3		0.2		0.49567	0.41567
			0.4		0.55659	0.43075
			0.8		0.59554	0.486757
0.2	0.3		0.1	0.4	0.42456	0.42654
				0.6	0.486436	0.456545
				0.8	0.55646	0.47678

Table 3
Outcomes $-\theta'(0)$ versus $\Pr, Nb, Nt, M, \lambda,$ and Bi for both cases linear and nonlinear stretching surface.

Parameters							$-\theta'(0)$
Pr	Nb	Nt	M	λ	Bi	$n = 1$	$n = 2$
3.0	0.2	0.3	0.1	0.1	0.4	0.36987	0.32786
4.0						0.39798	0.34768
5.0						0.41567	0.36757
	0.1	0.3	0.1	0.1	0.4	0.31876	0.27577
	0.4					0.29987	0.259807
	0.8					0.2688	0.2334
		0.1	0.1			0.3306	0.29676
		0.4				0.3180	0.25678
		0.8				0.2942	0.23678
			0.2			0.36877	0.30678
			0.8			0.34236	0.29979
			1.2			0.32765	0.279809
2				0.2	0.4	0.29988	0.29668
				0.6		0.30878	0.31857
				1.2		0.32977	0.32786
2					0.3	0.26774	0.33456
					0.5	0.30775	0.3738654
					0.8	0.356556	0.403452

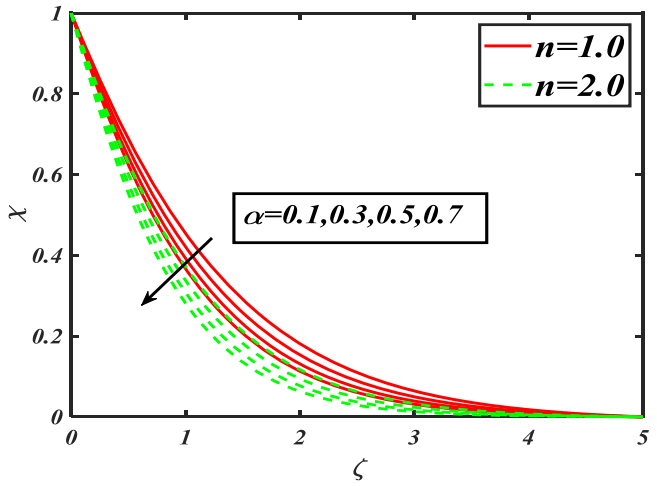

Fig. 18. fluctuation of velocity χ against α.

Table 4
Outcomes $-\varphi'(0)$ versus Pr, Nb, Nt, M and λ for both cases linear and nonlinear stretching surface.

Parameters					$-\varphi'(0)$	
Pr	Nb	Nt	M	λ	$n=1$	$n=2$
0.3	0.4	0.4	0.4	0.4	0.45566	0.46879
0.5					0.47456	0.49756
0.7					0.50768	0.50856
0.4	0.1	0.3			0.54689	0.85655
	0.5				0.610667	0.907879
	0.9				0.65889	0.95978
		0.1			0.62563	0.53678
		0.3			0.61668	0.51867
		0.7			0.58788	0.485768
			0.1		0.478678	0.49546
			0.5		0.436448	0.46436
			0.7		0.416778	0.4378
				0.3	0.429578	0.459876
				0.5	0.41895	0.43866
				0.7	0.408767	0.41678

Table 5
Outcomes motile microorganisms profile $-\chi'(0)$ versus λ, Pe, Rd, Lb, and M for both values($n=1$&2).

Parameters				$-\chi'(0)$	
λ	Pe	Lb	M	$n=1$	$n=2$
0.1	0.2	0.2	0.2	0.58765	0.64674
0.7				0.53678	0.6168
1.1				0.51688	0.59678
0.2	0.3	1	0.1	0.7013	0.65854
	0.5			0.757686	0.72567
	1.3			0.80689	0.78645
	0.1	0.3	0.1	0.7864676	0.605645
		0.7		0.85696	0.635436
		0.9		0.893563	0.67054
			0.1	0.686563	0.6810
			0.3	0.64546	0.65668
			0.9	0.62564	0.62978

Conclusions

The study explains the flow of Williamson nanofluid over linear and non-linear stretching surfaces with motile microorganisms as limiting factors. The numerical solution has been found by using bvp4c technique through MATLAB. The vital objectives of the current problem are discussed below as:

- The stretching ratio parameter falls for velocities concentration, volumetric concentration, temperature concentration and motile microorganism's concentration.
- The augmentation of magnetic parameter diminishes the both radial and azimuthal velocities of nanoparticles.
- The volumetric concentration of nanoparticles boosted with thermophoresis parameter and falls for Lewis number and Prandtl number.
- The higher valuation of both Peclet number and bioconvection Lewis number reduced the motile concentration of nanoparticles of fluid.

Acknowledgment

This work was supported the Natural Science Foundation of Zhejiang Province (Grant No. LQ19A010001).

References

[1] S.U. Choi, J.A. Eastman, *Enhancing the Thermal Conductivity of Fluids with Nanoparticles* (No. ANL/MSD/CP-84938; CONF-951135-29), Argonne National Lab., IL (United States), 1995.
[2] J. Buongiorno, Convective transport in nanofluids, J. Heat Transf. 128 (3) (2006) 240–250.
[3] M. Ramzan, A. Rafiq, J.D. Chung, S. Kadry, Y.M. Chu, Nanofluid flow with autocatalytic chemical reaction over a curved surface with nonlinear thermal radiation and slip condition, Sci. Rep. 10 (1) (2020) 1–13.
[4] R. Katta, P. Jayavel, Heat transfer enhancement in radiative peristaltic propulsion of nanofluid in the presence of induced magnetic field, Numer. Heat Transf., Part A: Appl. (2020) 1–28.
[5] M. Nazeer, M.I. Khan, M.U. Rafiq, N.B. Khan, Numerical and scale analysis of Eyring-Powell nanofluid towards a magnetized stretched Riga surface with entropy generation and internal resistance, Int. Commun. Heat Mass Transf. 119 (2020) 104968.
[6] M. Turkyilmazoglu, Single phase nanofluids in fluid mechanics and their hydrodynamic linear stability analysis, Comput. Methods Programs Biomed. 187 (2020) 105171.
[7] R. Ellahi, F. Hussain, S.A. Abbas, M.M. Sarafraz, M. Goodarzi, M.S. Shadloo, Study of two-phase newtonian nanofluid flow hybrid with hafnium particles under the effects of slip, Inventions 5 (1) (2020) 6.
[8] S. Qayyum, M. Ijaz Khan, T. Hayat, A. Alsaedi, M. Tamoor, Entropy generation in dissipative flow of Williamson fluid between two rotating disks, Int. J. Heat Mass Transf. 127 (2018) 933–942.
[9] W. Ibrahim, Magnetohydrodynamics (MHD) flow of a tangent hyperbolic fluid with nanoparticles past a stretching sheet with second order slip and convective boundary condition, Res. phys. 7 (2017) 3723–3731.
[10] Muhammad Usman Ashraf, Muhammad Qasim, Abderrahim Wakif, Muhammad Idrees Afridi, Isaac L. Animasaun, A generalized differential quadrature algorithm for simulating magnetohydrodynamic peristaltic flow of blood-based nanofluid containing magnetite nanoparticles: a physiological application, Numer. Methods Partial Differ. Eq. (2020) https://doi.org/, doi:10.1002/num.22676.
[11] M.Ijaz Khan, Transportation of hybrid nanoparticles in forced convective Darcy-Forchheimer flow by a rotating disk, Int. Commun. Heat Mass Transf. 122 (March 2021) 105177.
[12] M. Turkyilmazoglu, Single phase nanofluids in fluid mechanics and their hydrodynamic linear stability analysis, Comput. Methods Programs Biomed. 187 (2020) 105171.
[13] Muhammad Ijaz Khan, Faris Alzahrani, Dynamics of activation energy and nonlinear mixed convection in Darcy-Forchheimer radiated flow of Carreau nanofluid near stagnation point region, J. Thermal Sci. Eng. Appl.1-20 (2021).
[14] Muhammad Ibrahim, M.Ijaz Khan, Mathematical modeling and analysis of SWCNT-Water and MWCNT-Water flow over a stretchable sheet, Comput. Methods Programs Biomed. 187 (April 2020) 105222.
[15] S.M. Atif, S. Hussain, M. Sagheer, The magnetohydrodynamic stratified bioconvective flow of micropolar nanofluid due to gyrotactic microorganisms, AIP Adv. 9 (2) (2019) 025208.
[16] K. Hosseinzadeh, S. Salehi, M.R. Mardani, F.Y. Mahmoudi, M. Waqas, D.D. Ganji, Investigation of nano-Bioconvective fluid motile microorganism and nanoparticle flow by considering MHD and thermal radiation, Inf. Med. Unlocked (2020) 100462.
[17] H. Waqas, S.U. Khan, M. Imran, M.M. Bhatti, Thermally developed Falkner–Skan bioconvection flow of a magnetized nanofluid in the presence of a motile gyrotactic microorganism: buongiorno's nanofluid model, Phys. Scr. 94 (11) (2019) 115304.
[18] S.U. Khan, A. Rauf, S.A. Shehzad, Z. Abbas, T. Javed, Study of bioconvection flow in Oldroyd-B nanofluid with motile organisms and effective Prandtl approach, Phys. A 527 (2019) 121179.
[19] A.S. Alshomrani, M. Ramzan, The upshot of the magnetic dipole on the flow of nanofluid along a stretched cylinder with gyrotactic microorganism in a stratified medium, Phys. Scr. (2019).
[20] A.M. Alwatban, S.U. Khan, H. Waqas, I. Tlili, Interaction of Wu's slip features in bioconvection of Eyring Powell nanoparticles with activation energy, Processes 7 (11) (2019) 859.
[21] I. Tlili, H. Waqas, A. Almaneea, S.U. Khan, M. Imran, Activation energy and second-order slip in bioconvection of Oldroyd-B nanofluid over a stretching cylinder: a proposed mathematical model, Processes 7 (12) (2019) 914.
[22] H. Waqas, S.A. Shehzad, S.U. Khan, M. Imran, Novel numerical computations on flow of nanoparticles in porous rotating disk with multiple slip effects and microorganisms, J. Nanofluids 8 (7) (2019) 1423–1432.
[23] M. Ramzan, H. Gul, J.D. Chung, S. Kadry, Y.M. Chu, Significance of Hall effect and Ion slip in a three-dimensional bioconvective Tangent hyperbolic nanofluid flow subject to Arrhenius activation energy, Sci. Rep. 10 (1) (2020) 1-.